

## Laboratory astrochemistry and modelling

# Processing of astrophysical ices by soft X-rays and swift ions

Sergio Pilling<sup>1,2</sup>

<sup>1</sup>Universidade do Vale do Paraíba (UNIVAP) / Laboratório de Astroquímica e Astrobiologia (LASA), Av. Shishima Hifumi, 2991, CEP: 12244-000, Sao Jose dos Campos, SP, Brazil.  
email: [sergiopilling@yahoo.com.br](mailto:sergiopilling@yahoo.com.br)

<sup>2</sup>Instituto Tecnológico de Aeronáutica - ITA / DCTA, Praça Marechal Eduardo Gomes, 50, CEP:12228-900, São José dos Campos, SP, Brazil.

**Abstract.** The employment of soft X-rays and swift ions has been used in laboratory to simulate the physicochemical processing of astrophysical ice analogs by energetic photons and cosmic rays. This processing includes excitation, ionization and molecular dissociation, desorption, as well as triggers the formation of new compounds. Here we present some results from experiments employing infrared spectroscopy in two different laboratories: LNLS/CNPEN in Campinas/Brazil and GANIL/CIRIL/CIMAP in Caen/France. Among the results are the formation of alkenes and aromatic compounds during the irradiation of saturated hydrocarbon-containing ices by cosmic ray analogs, the production of the nucleobase adenine during soft X-ray photolysis of N<sub>2</sub>:CH<sub>4</sub> ice, as well as the formation of peptide bonds during the bombardment of frozen glycine by cosmic ray analogs. The interaction between cosmic ray analogs and ionizing soft X-rays probed in the laboratory allows us to identify reaction routes that lead to chemistry enhancement of astrophysical ices and help us put constraints in prebiotic chemistry.

**Keywords.** Laboratory measurements, X-rays, Cosmic-rays, Astrophysical ices, FTIR, Astrochemistry, Astrobiology

---

## 1. Introduction

The birthplace of stars is the densest and coldest place of the interstellar medium (ISM) called dense molecular clouds. These regions have typical gas densities of 10<sup>3</sup>-10<sup>8</sup> atoms cm<sup>-3</sup> and temperatures in the order of 10-50 K. Because of the low temperature, dust particles (mainly silicates and carbonaceous compounds such as amorphous C and SiC) can accrete molecules from the gas phase and become coated with an ice mantle. The interstellar ice mantles (or simply interstellar ices) consist primarily of amorphous H<sub>2</sub>O, but usually also contain a variety of other simple molecules, such as CO<sub>2</sub>, CO, CH<sub>3</sub>OH, and NH<sub>3</sub> (e.g., Ehrenfreund & Charnley 2000; Gibb *et al.* 2001; Boogert *et al.* 2004).

Laboratory studies and astronomical observations indicate that photolysis and radiolysis of such ices can create complex organic compounds, and even prebiotic molecules such as amino acids and nucleobases (e.g. Maloney *et al.* 1996; Bernstein *et al.* 2002; Muñoz Caro *et al.* 2002; Kobayashi *et al.* 2008; Pilling *et al.* 2009 Vasconcelos *et al.* 2017a, b, c). Figure 1 illustrates the scenario in which such cosmic rays, soft X-rays and fast electrons induce chemical changes in the icy environments.

Inside dense regions of the interstellar medium, where direct stellar UV is extremely attenuated, X-rays (despite some degree of attenuation) and cosmic rays are the main drivers of the gas phase and grain surface chemistry. For example, the penetration depth of 46 MeV Ni ions and equivelocity protons inside water ice is about 1 and 3 orders of magnitude higher than for 500 and 50 eV photons (considering the photoabsorption

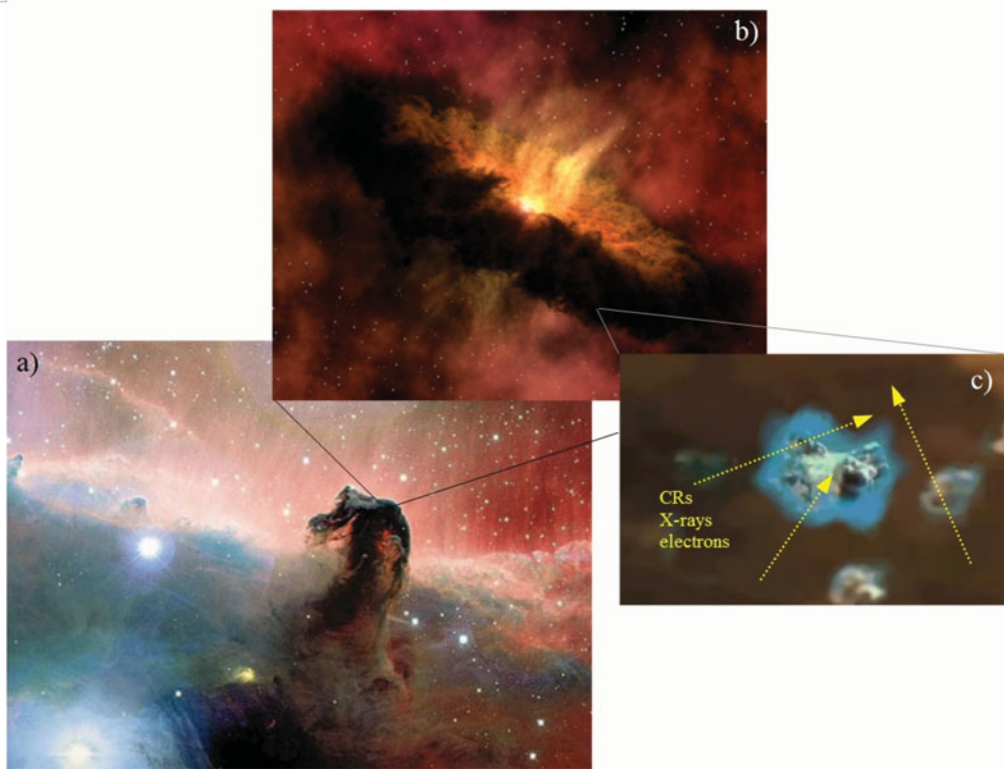


**Figure 1.** Mosaic with and schematic representation of the interaction between ionizing agents with interstellar grains inside dense clouds. A). Picture of the Horsehead Nebula, a dark molecular cloud, roughly 1,500 light years distant, embedded in the vast and complex Orion Nebula (Credit: Jean-Charles Cuillandre (CFHT), Hawaiian Starlight, CFHT. source: <http://www.nasa.gov>). b) Artist impression of a protostellar disk around a recently formed or forming star. (Credit: NASA/JPL-Caltech/R. Hurt -SSC). C) Illustration of interstellar grains covered with an ice cap being processed by ionizing radiation (Cosmic rays, X-rays and electrons).

cross-section from Chan *et al.* (1993) and McLaren *et al.* (1987)). In these environments, the dust grains can reach a size in the order of a micron, as a coagulation of sub-micron grains occurs with ice-rich mantles from tens of nanometers to tens of microns (Li & Greenberg 1997; Taylor *et al.* 1996; Witt *et al.* 2001; and references therein).

The desorption induced by energetic radiation is another important process that modifies the chemical abundances in the gas phase in space environments, mainly in cold and denser regions (see e.g. Prasad & Tarafdar 1983; Brown *et al.* 1984; Shen *et al.* 2004; Bonfim *et al.* 2017). As indicated by Shen *et al.* (2004), in the case of cosmic ray particles, the sputtering produced by direct impact and whole grain heating (classical sublimation) due to energy deposition in the bulk are also two efficient processes for releasing molecules from frozen surfaces to the gas phase.

Bonfim *et al.* (2017) pointed out, in a theoretical-experimental study employing X-rays on ices (broadband X-ray processing of SO<sub>2</sub> ice at 12 K), that the X-ray photodesorption yield (upper limit) is around 0.25 molecules/photon, which is between 100 and 1000 times higher than the one from Öberg *et al.* (2009), comparing with values obtained for CO and N<sub>2</sub> employing UV photons. The desorption (or sputtering) induced by swift ions in ices is several orders of magnitude higher than the one produced by ionizing photons and can

reach values around 10000 molecules/impact (Brown *et al.* 1984; Baragiola *et al.* 2003; Pilling *et al.* 2010a), and as discussed by Rocha *et al.* (2017), may be also dependent on ice polarity (ices composed of polar molecules are more resistant to destruction, whereas apolar molecule-containing ices are more easily destroyed). Additionally, it has been observed that the number of molecules ejected after ion impact scale with the square of the electronic projectile energy loss (Seperuelo-Duarte *et al.* 2010; Dartois *et al.* 2015; Mejía *et al.* 2015).

The processing of astrophysical ices by ionizing radiation such as soft X-rays and swift ions has been used in laboratory to simulate the effects of energetic photons (e.g. Pilling *et al.* 2009; Chen *et al.* 2013; Pilling *et al.* 2011b; Pilling & Bergantini 2015; Jimenes-Escobar *et al.* 2016; Vasconcelos *et al.* 2017c; Bonfim *et al.* 2016; Rachid *et al.* 2017; Almeida *et al.* 2014; and references therein) and cosmic rays (e.g. Strazzulla *et al.* 1983; Palumbo 2006; Strazzulla *et al.* 2007; Seperuelo-Duarte *et al.* 2009; Pilling *et al.* 2010a, 2010b; Hijazi *et al.* 2011; Andrade *et al.* 2013; Bergantini *et al.* 2014a; de Barros *et al.* 2014; Mejía *et al.* 2014; Almeida *et al.* 2017).

## 2. Experimental methodology

Over the years, several physicochemical techniques have been employed to study the surfaces and the bulk of astrophysical ices exposed to radiation (e.g. Thermal Programmed Desorption TPD, X-rays Spectroscopy XAS, Stimulations Ion Desorption SID, Plasma Desorption PD, Infrared Spectroscopy, and others). Here, we will focus on the study of the bulk of simulated ice by employing infrared (IR) spectroscopy in transmission mode (Fourier Transformed IR spectroscopy FTIR). Basically, the methodology employed requires two high-vacuum chambers (one to prepare the gas mixture of astrophysical interest and another to produce the icy film and perform the irradiation/bombardment), a helium cryostat, an ionization source and an infrared spectrometer that can operate in reflection or transmission mode. More details of such technique can be seen elsewhere (e.g. Seperuelo Duarte *et al.* 2009, 2010; Pilling *et al.* 2010a,b; Portugal *et al.* 2014; Pilling & Bergantini 2015, and references therein).

The highlight experiments described in this manuscript were performed employing two similar high-vacuum chambers at two different laboratories: the Brazilian Synchrotron light source (LNLS/CNPEM) in Campinas/Brazil, and the Grand Accélérateur d'Ion Lourdes (GANIL/CIRIL/CIMAP) in Caen/France. Briefly, the gaseous samples were inserted in the mixed chamber and the gas mixture was prepared in proportions similar to those observed in space environments (e.g. ices at protoplanetary disks PPDs, surface of Jovian moons, comets, etc.). For pure samples, only one type of compound is used. Basically, the pressure inside the mixed chamber is in the order of 10-100 mbars during sample preparation. The gas mixture (or pure sample) is usually inserted slowly into the main chamber through an inlet needle with its end close to the IR-transparent cold substrate (e.g. ZnSe, KBr or CaF<sub>2</sub>) resulting in ice film formation (~ 0.02-0.1 micron min<sup>-1</sup>). The icy sample has thickness usually from 0.1-2 microns, but depending on the experiments a very thin or very thick sample can be produced. The base pressure of the main chamber is around 10<sup>-9</sup> mbar and during the irradiation stage itself the chamber pressure can increase a little due to sputtering processes and reaches 10<sup>-8</sup> mbar. After ice production, an infrared spectrum is obtained to characterize the sample and its thickness. The molecular column densities and ice thickness of samples were determined from the relation between the measured IR band area of a given vibrational mode in the IR spectrum and its respective band strength, B (cm molecule<sup>-1</sup>) and average number density of ice, both taken from literature (see details at Pilling 2010a, 2010b, 2011a;

Portugal *et al.* 2014; Pilling & Bergantini 2015 and references therein). The in-situ IR spectra were recorded for ices irradiated at different fluences using FTIR spectrometer (e.g. Agilent Carry 630 or Nicolet Magna 550) from 4000 to 600  $\text{cm}^{-1}$  with 1-2  $\text{cm}^{-1}$  resolution. A background spectrum allowing the absorbance measurements was collected before gas deposition. As described, for example, by Pilling *et al.* (2010a) and Pilling & Bergantini (2015), in such experiments, the sample cryostat system can be rotated over 180 degrees and fixed at three different positions to allow gas deposition, FTIR measurement and ice exposure to the radiation beam.

From the analysis of the evolution of IR bands as a function of radiation fluence we derive molecular parameters such as effective destruction cross sections (for parent species) and effective formation cross section (for daughter species) as described in details elsewhere (e.g. Seperuelo Duarte *et al.* 2009; Pilling 2010a, Portugal *et al.* 2014; Pilling and Bergantini 2015 and references therein). Additionally, the desorption yield and molecular branching ratio at chemical equilibrium can be determined (e.g. Bonfim *et al.* 2017, Almeida *et al.* 2017; Rachid *et al.* 2017; Vasconcelos 2017a,b). Such chemical equilibrium occurs at a large radiation fluence and the composition of the sample, kept a constant temperature, stays constant even if the sample continues to be exposed to radiation. With such parameters, we can estimate the reaction rates and the half-life of parent species, as well as the yield of new compounds produced in the ices in astrophysical environments by knowing the radiation flux in space (e.g. Pilling 2010a; Pilling and Bergantini 2015; Rachid *et al.* 2017, and references therein).

### *X-ray induced processes in ices*

In general, as discussed by Gullikson & Henke (1989) and Pilling & Bergantini (2015), X-ray absorption occurs via the photoelectric effect so that it results in the generation of a photoelectron with energy  $E = h\nu - E_b$ , where  $h\nu$  is the soft X-ray photon energy (in this work 100  $\leq h\nu$  (eV)  $\leq$  2000) and  $E_b$  is the binding energy of the electron. Electron binding energy is a generic term for the ionization energy that can be used for species with any charge state. For the species containing CHONS atoms, the highest electron binding energy within the available photon energy range is found for O K-edge electrons ( $\sim$  540 eV), followed by N K-edge electrons ( $\sim$  400 eV), C K-edge electrons ( $\sim$  290 eV), and S L-edge electrons ( $\sim$ 160 eV). Additionally, the weakest electron binding energies come from the valence electrons of  $\text{NH}_3$  ( $\sim$  10 eV), followed by valence electrons of  $\text{SO}_2$  (12.3 eV),  $\text{H}_2\text{O}$  (12.6 eV), and  $\text{CO}_2$  (13.7 eV). The effect of soft X-ray-induced secondary electrons has been studied by several groups in the literature (e.g., Henke *et al.* 1979; Gullikson & Henke 1989; Akkerman *et al.* 1993; Hufner 1995; Cazaux 2006; Pilling *et al.* 2009; Pilling & Andrade 2012) and is a rather complex process.

As discussed by Pilling & Bergantini (2015), a simplified description for the interaction of soft X-ray with astrophysical ices can be divided into four steps: **i)** First, photoabsorption of X-ray and the generation of energetic primary electrons (see above). Such fast primary electrons lose energy by creating electron-hole pairs at a distance that is generally short compared with the penetration depth  $L$  of the incoming photon. As indicated by Bergantini *et al.* (2014b), the range of 1 keV electrons is around 60 nm inside such astrophysical analog samples and for low-energy electrons ( $\sim$  5 eV), the mean-free path inside such ices is around 1-2 nm; **ii)** Excitation of secondary electrons by fast primary electrons (photoelectrons). Once a secondary electron is created, it will undergo a short random walk in the material while losing energy due to the creation of phonons. Moreover, following Gullikson & Henke (1989), each soft X-ray may induce tens of secondary electrons inside matter, and this number increases as the temperature of the target increases; **iii)** Transport of the secondary electrons, including energy, to the lattice. Following Henke

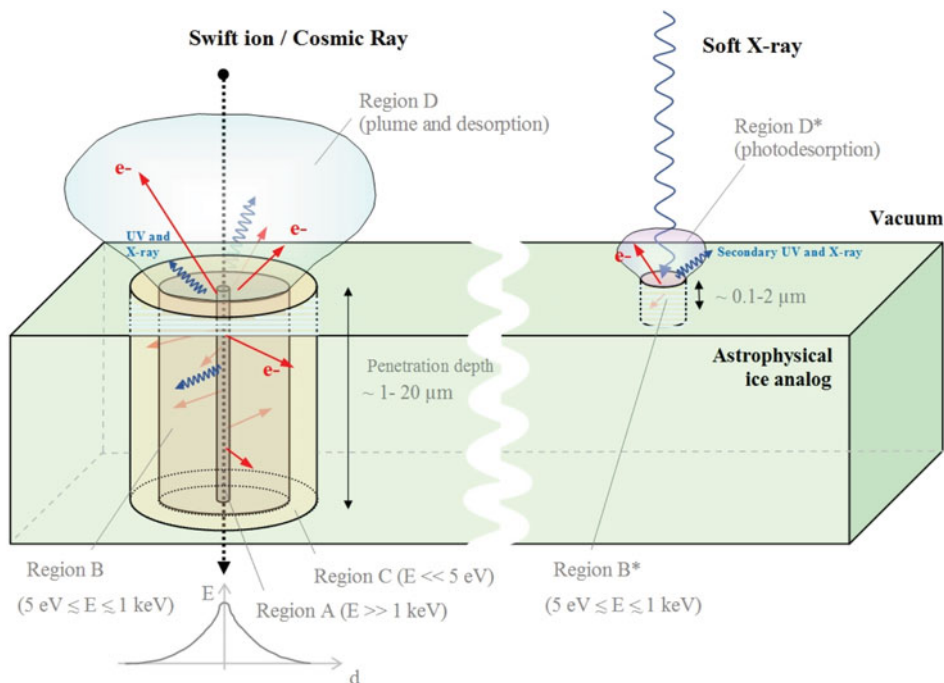


**Figure 2.** Schematic diagram of the different physicochemical regions surrounding the ion and photon track during processing of the typical astrophysical ice by cosmic rays and soft X-rays). Adapted from Vasconcelos *et al.* (2017c).

*et al.* (1979), most secondary electrons have energies below 5 eV. When captured by a molecular target inside the bulk, such electrons can induce further molecular dissociation, for example, via the dissociative electron attachment mechanism ( $AB + e^- \rightarrow AB^- \rightarrow A^- + B$ ). The mean-free path of such secondary electrons is much reduced in comparison to photoelectrons, and its yield can vary depending on sample density and temperature; and **iv**) Escape of secondary electrons reaching the surface with sufficient energy to overcome any potential barrier at the surface or be thermalized/captured by any molecular species or center in the bulk. In astrophysical water-rich ices (insulators), a secondary electron will undergo many collisions before it either escapes through the surface or loses enough energy so that it is unable to escape or becomes trapped by interacting with a center in the bulk.

#### *Cosmic-ray induced processes in ices*

The energy provided by the incoming swift oxygen ions and the energy delivered by the incoming soft photons induce different physicochemical processing inside the ice as illustrated in Figure 2. Its main difference comes from the radial energy gradient centered at the ion track compared to photons. For example, in the case of ion bombardment, we can identify four distinct regions (e.g. Portugal *et al.* 2014; Vasconcelos *et al.* 2017c): **Region A** (track core region) - A small cylindrical region, along the ion track in which the energy delivered is extremely high ( $E \gg 1$  keV); with complete ionization and thus destruction of molecules along the track; **Region B** (ionization/dissociation region) - A cylindrical surrounding region A, in which the energy is not enough ( $1\text{keV} \geq E \geq 5$  eV) to atomize the target but induces bond ruptures (dissociation) and target electron ejection (ionization). Primary electrons and subsequent secondary electrons are a source of energy input for chemical reactions inside this region. As pointed out by Vasconcelos

*et al.* (2017c), after ion bombardment on N<sub>2</sub>:CH<sub>4</sub> ices, the molecules within this region can be converted to radicals that may react to produce new species such as (C<sub>2</sub>H<sub>2</sub>, C<sub>2</sub>H<sub>4</sub>, C<sub>2</sub>H<sub>6</sub>, HCN, HNC, NH<sub>3</sub>, N<sub>3</sub>, and others); **Region C** (region of morphological changes) - A region far from the ion track, in which not very much energy is available ( $E \ll 5$  keV), where only morphological changes are induced in the astrophysical-like frozen sample, such as change in the crystalline structure; and **Region D** - A plume-like shaped region outside the surface that contains ejected lost electron, ions, neutral atoms, and molecular clusters sputtered from the sample. Due to atomic and molecular deexcitation, UV and soft X-rays may also be released in this region. Some reactions in the gas phase may occur inside this region due to molecular excitation, local density and energy available.

For X-rays, the volume of processed ice by incoming photon is smaller and, as illustrated in Fig. 2, two distinct regions in terms of physicochemical processes can be identified. They are: **Region B\*** (photoionization/photodesorption) where bond ruptures (dissociation) and electron ejection (photoionization) happen. Inside this region, the incoming photons (broadband soft X-rays with energies from 6 to 2000 eV) induce ejection of electrons, which trigger several chemical reaction routes; and **Region D\*** - A plume-like shaped region outside the surface which contains photodesorption products, for example, photoelectrons, ejected ionic and atomic species, and molecules sputtered from the sample (less pronounced than in the case of ion bombardment). Contrary to ion bombardment experiments, no molecular clusters are expected to desorb from the surface. According to Vasconcelos *et al.* (2017c), both ionizing agents (swift ions and soft X-rays) produce the same kind of new species during ice processing with different production efficiencies and equilibrium branching ratio - EBR (reached after a longer radiation fluence). More details about EBR of irradiated ices is given elsewhere (e.g. Almeida *et al.* 2017; Rachid *et al.* 2017).

### 3. Experiments highlights

#### 3.1. Production of nucleobase adenine and nitriles during soft X-rays photolysis of N<sub>2</sub>:CH<sub>4</sub> ices

Pilling *et al.* (2009) presented, for the first time, the chemical alteration produced by the interaction of broad band soft X-rays (in the 0.5-3 keV range), and its induced primary and secondary electrons, on N<sub>2</sub>:CH<sub>4</sub> (95:5) ice at 15 K in an attempt to simulate the photochemistry induced in the frozen surface of outer solar system bodies such as Pluto, Triton and other KBOs (Kuiper belt objects), as well as in the surface of aerosols in the upper atmosphere of the Saturn moon, Titan. The experiments have been performed in a high-vacuum chamber coupled to the SXS beamline SXS at LNLS/CNPEM. In-situ sample analyses were performed by an FTIR spectrometer.

Concerning the applicability of results in Titan chemistry, according to the authors, the experiments simulated roughly  $7 \times 10^6$  years of solar soft X-ray exposure on Titan atmosphere. Besides the parent species N<sub>2</sub> and CH<sub>4</sub>, the ice sample had also a small amount of water and CO ice (less than 1%), which simulates periods of heavy cometary bombardment on such solar system bodies. The in-situ IR analysis showed several organic molecules created and trapped in the ice at  $\sim 15$  K, including the reactive cyanate ion OCN<sup>-</sup>, nitriles, and possibly amides and esters. The authors also observed that the thermal heating of a frozen sample drastically changes its chemistry, resulting in an organic residue rich in C-C and C-N aromatic structures. Ex-situ Gas Chromatography (GC-MS) and H-NMR analysis of the organic residue at room temperature (300 K) showed that among several nitrogen compounds, adenine (C<sub>5</sub>H<sub>5</sub>N<sub>5</sub>), one of the

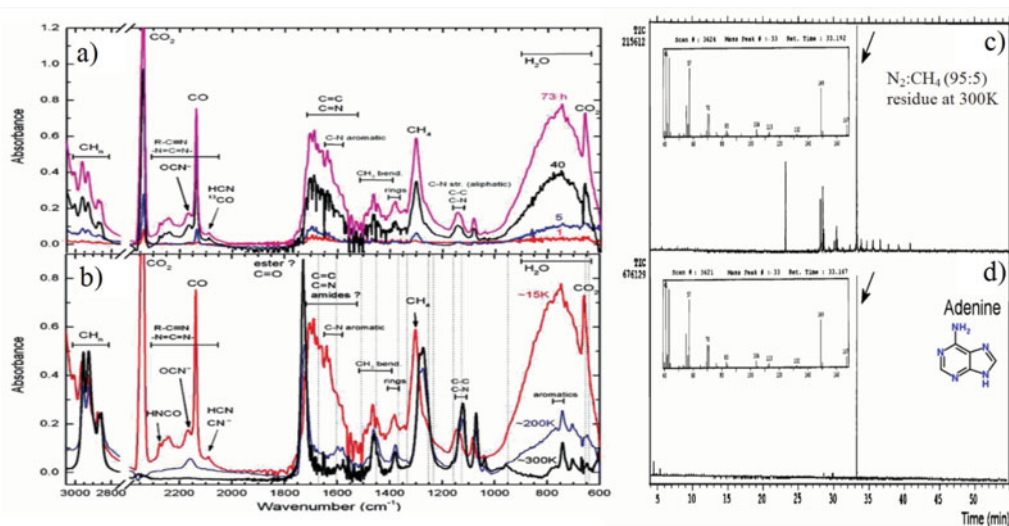


**Figure 3.** FTIR spectra of the irradiated  $\text{N}_2:\text{CH}_4$  (95:5) ice at 15 K by soft X-rays: a) Evolution of spectral features as a function of irradiation time (1 h  $\sim 3 \times 10^{10}$  erg  $\text{cm}^2$ ). b) Comparison between FTIR spectra of a 73 h irradiated sample at 15, 200, and 300 K. The vertical dashed lines indicate the frequency of some vibration modes of crystalline adenine. The total-ion current chromatogram obtained after the derivatization process of the ice residue at 300 K, and adenine standard are given in panels c) and b), respectively. The inset figures are the mass fragmentation of the sample and the adenine derivative at the retention time of around 33.2 min (arrows). Adapted from Pilling *et al.* (2009).

DNA-nucleobases, is one of the most abundant species produced due to irradiation by soft X-rays. The FTIR spectra of the irradiated  $\text{N}_2:\text{CH}_4$  (95:5) ice at 15 K by soft X-rays, as well as, ex-situ analysis of the organic residue by GC-MC, are presented in Figure 3.

Vasconcelos *et al.* (2017c), in a similar experiment employing the SGM beamline of the LNL/CNPEM, observed the production of several new organic molecules, including hydrocarbons and nitriles. Among the daughter species identified were  $\text{C}_2\text{H}_2$ ,  $\text{C}_2\text{H}_4$ ,  $\text{C}_2\text{H}_6$ , HCN, HNC,  $\text{NH}_3$ , and  $\text{N}_3$  (the most abundant one). In this experiments, the broadband X-ray beam from 6 to 2000 eV was employed. The authors have also measured the effective dissociation cross-sections for  $\text{CH}_4$  and  $\text{N}_2$  at 12 K and the values obtained were  $3.7 \times 10^{-19}$   $\text{cm}^2$  and about  $3.8 \times 10^{-19}$   $\text{cm}^2$ , respectively. A comparison with a similar experiment, but employing swift ions (15.7 MeV  $\text{O}^{+5}$ ) as the ionizing agent shows that cross section is roughly 6 orders of magnitude higher ( $\sim 10^{-13}$   $\text{cm}^2$ ) in case of ion bombardment. The authors also observe that molecular synthesis is strongly enhanced for swift ions in comparison to soft X-rays of the same energy fluence deposited and the results suggest that the modeling of the abundance of astrophysical ices over long periods of time may provide insights into the ion and photon chemistry present in the surface of space environments, such as in objects of the outer Solar System.

This investigation confirms previous studies suggesting that the organic chemistry in the outer solar system bodies such as KBO, Pluto and triton, as well as in Titan atmosphere (aerosols) and on its surface, should be highly complex, being rich in prebiotic molecules involving nitriles, adenine and other compounds. Molecules such as these on the early Earth have found a place that allows life (as we know it) to flourish, a place with liquid water. Additionally, it was observed that the stability of nucleobases in the presence of X-rays is very enhanced in comparison to the stability of amino acids allowing

this species an extended half-life in astrophysical environments (Pilling *et al.* 2011b and references therein).

### 3.2. Appearance of peptide bonds during the bombardment of frozen glycine by cosmic rays

The study of glycine molecule stability in the crystalline zwitterion form, known as  $\alpha$ -glycine ( $^+\text{NH}_3\text{CH}_2\text{COO}^-$ ), under the action of heavy cosmic ray analogues, was performed by Portugal *et al.* (2014). The samples were bombarded at two temperatures (14 and 300 K) by  $^{58}\text{Ni}^{11+}$  ions with energies of 46 MeV, up to a final fluence of  $10^{13}$  ion  $\text{cm}^{-2}$ , inside a high-vacuum chamber at the heavy-ion accelerator GANIL. Cosmic ray processing of the sample shows the production of several daughter species, such as  $\text{OCN}^-$ , CO,  $\text{CO}_2$  and  $\text{CN}^-$  and also suggests the appearance of peptide bonds (amide bonds at 1660, 1600 and 1320  $\text{cm}^{-1}$ ; Reis *et al.* 2006; Kaiser *et al.* 2013) during irradiation as presented in Figure 4. Selected reaction pathways for some daughter species, as well as the suggested peptide bond formation that can occur in region B and a schematic plot of the energy delivered within the sample as a function of the distance of the ion track, are also shown. The peptide bond occurs by the link between the carboxyl group of one amino acid and the amine group of another amino acid, forming an amide group with the release of a water molecule. Such intermolecular bonds between amino acids provide the basis for the production of longer molecular chains, including proteins.

The estimated half-life of glycine in the interstellar medium and in the Solar System in the presence of cosmic rays was around  $3\text{--}8 \times 10^3$  yr and  $0.8\text{--}4 \times 10^3$  yr, respectively. As also discussed by Pilling *et al.* (2014), in one experiment employing fast electrons in solid glycine, the survivability of glycine is highly increased if the samples are at 300 K when compared to low temperature experiments at 14 K due to the presence of free radicals (radiolysis products) in the ice which participate on further reaction pathways consuming the parent species.

Additionally, Portugal *et al.* (2014) suggested that glycine could be present in space environments that suffered aqueous changes, such as the interiors of comets, meteorites and planetesimals. This molecule is present in the proteins of all living beings. Therefore, studying its stability in these environments will provide further understanding of the role of this species in the prebiotic chemistry on Earth.

Pilling *et al.* (2013), in another experiment bombarding solid glycine with ions, have also observed a small feature around 1650–1700  $\text{cm}^{-1}$ , tentatively attributed to an amide functional group, which was observed in the IR spectra of irradiated samples, suggesting that cosmic rays may induce peptide bond synthesis in glycine crystals. In such experiments, they have observed and quantified the selective destruction of glycine-bonds employing 1 MeV protons. They observed that the N-H bond was the most sensitive to incoming ions in two types of solid glycine at room temperature ( $\alpha$ - and  $\beta$ -glycine). The authors estimated that the half-lives of  $\alpha$ -glycine and  $\beta$ -glycine zwitterionic forms bombarded by 1 MeV protons at room temperature, extrapolated to the Earth orbit environment, were  $9 \times 10^5$  and  $4 \times 10^6$  years, respectively. In the diffuse interstellar medium, the estimated values are 1 order of magnitude lower. The results suggest that the pristine interstellar  $\beta$ -glycine form should be the most probable kind of glycine polymorph to survive hostile space radiation environments. Combining this result with the fact that this compound has the higher solubility among the other glycine polymorphs, the authors suggest that the  $\beta$ -glycine polymorph was relevant for the production of the first peptides on early Earth.

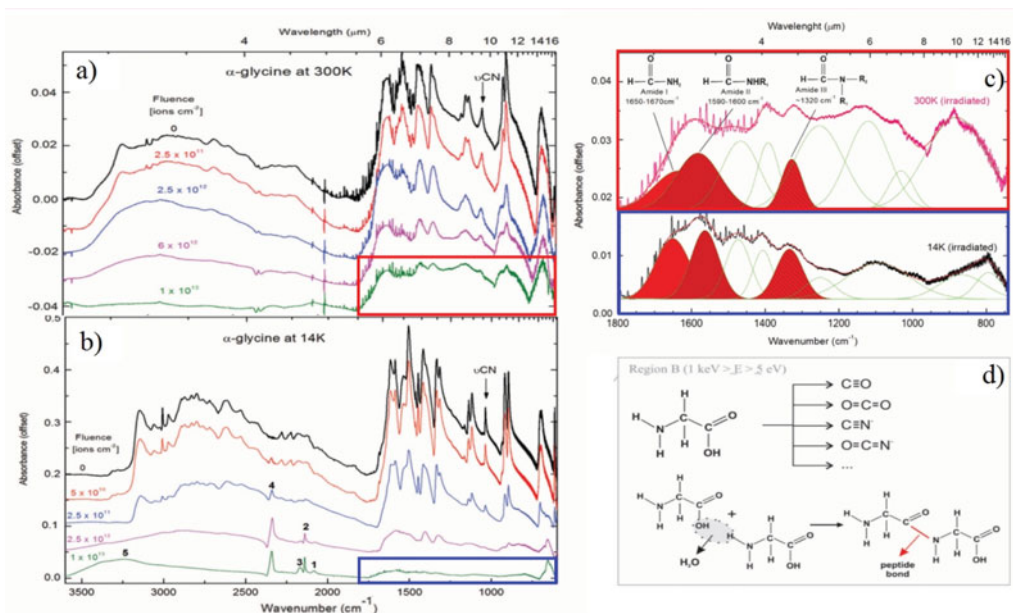


**Figure 4.** Processing of glycine by cosmic rays and formation of peptide bonds. Panels a and b show the IR spectra of  $\alpha$ -glycine before (top dark line) and after different irradiation fluences. The peaks of daughter species formed are indicated by numbers: (1)  $\text{CN}^-$  ( $2080\text{ cm}^{-1}$ ); (2)  $\text{CO}$  ( $2137\text{ cm}^{-1}$ ); (3)  $\text{OCN}^-$  ( $2165\text{ cm}^{-1}$ ); (4)  $\text{CO}_2$  ( $2336\text{ cm}^{-1}$ ); (5)  $\text{H}_2\text{O}$  ( $3280\text{ cm}^{-1}$ ). Panel c shows an expanded view of IR spectra of the residues produced after the bombardment employing the fluence of  $10^{13}\text{ Ni ion cm}^{-2}$ . Filled curves present tentative assignments of amide bands obtained from a spectral deconvolution employing nine Gaussian profiles, in the range  $1800\text{--}750\text{ cm}^{-1}$ . A scheme of peptide bond formation is presented in panel d. Adapted from Portugal *et al.* (2014).

### 3.3. Formation of alkenes and aromatic compounds by cosmic rays

The formation of  $\text{C}=\text{C}$  and  $\text{C}\equiv\text{C}$  bonds from the processing of pure  $c\text{-C}_6\text{H}_{12}$  (cyclohexane) and mixed  $\text{H}_2\text{O}:\text{NH}_3:c\text{-C}_6\text{H}_{12}$  (1:0.3:0.7) ices at 13 K by highly charged and energetic ions (219 MeV  $\text{O}^{7+}$  and 632 MeV  $\text{Ni}^{24+}$ ) was experimentally studied by Pilling *et al.* (2012). The measurements were performed inside a high-vacuum chamber at GANIL and simulate the physical chemistry induced by medium-mass and heavy-ion cosmic rays in interstellar ice analogues. In situ analysis was performed by a Fourier transform infrared spectrometry at different ion fluences.

According to the authors, for the experiment involving the mixed ice bombarded by heavy-ion cosmic ray analogues the determined dissociation cross-sections of  $\text{H}_2\text{O}$ ,  $\text{NH}_3$  and  $c\text{-C}_6\text{H}_{12}$  are between  $2\text{--}3 \times 10^{-13}\text{ cm}^2$ . The results indicate that the effective dissociation cross-section of cyclohexane is about one order of magnitude higher when swift heavy cosmic ray analogues were employed in comparison to the experiment employing medium-mass cosmic rays. Additionally, they observed that the radiolysis of simple alkanes such as cyclohexane in astrophysical ice analogues are consistent with the production of unsaturated molecules containing double bonds, triple bonds (e.g.  $2334\text{ cm}^{-1}$ ) and/or ring(s) (e.g.  $3085\text{ cm}^{-1}$ ). Extrapolating to an astrophysical scenario, the maximum production of alkenes is obtained after about  $3\text{--}5 \times 10^6\text{ yr}$  independent of the projectile type and the presence of polar species in the ice (e.g. water and ammonia). The authors also observed that effective formation cross-sections of alkenes, considering the C-H out-of-plane bending mode at  $719\text{ cm}^{-1}$  (band strength,  $B \sim 8 \times 10^{-18}\text{ cm molecule}^{-1}$ ), in the pure  $c\text{-C}_6\text{H}_{12}$  ice and mixed ice were about  $10^{-15}$  and  $10^{-14}\text{ cm}^2$ , respectively. The

maximum value was roughly the same for both experiments,  $10^{-2}$  alkenes per cyclohexane molecule irradiated by a cosmic ray analogue. Another consequence of this induced unsaturation is the production of molecular hydrogen in the ice, which can be released to the gas phase (desorbed) depending on its energy or ice temperature.

Finally, the authors found that the  $3.4 \mu\text{m}$  band detected in the IR spectrum of Planetary nebulae PN IRAS 05341+0852 is very similar to the band observed for the organic residue (at  $\sim 130 \text{ K}$ ) obtained after ion bombardment of the  $\text{H}_2\text{O}:\text{NH}_3:\text{c-C}_6\text{H}_{12}$  ice. This suggests two different issues: first, it puts a constraint in the temperature of dust grains in the region, and secondly, it also indicates that a negligible amount of CO was initially present in the grains. Additionally, considering the sharp  $3.37 \mu\text{m}$  absorption peak (C-H asymmetric stretching mode in  $-\text{CH}_3$ ), they suggested that grains at the astronomical objects PPN CRL 618, DISM GC IRS 6E and at the Murchison carbonaceous meteorite were probably exposed to heavy cosmic rays with fluence higher than  $3 \times 10^{13} \text{ ions cm}^{-2}$  or to some kind of ionizing agent that delivered an energy dose higher than  $2 \times 10^8 \text{ J kg}^{-1}$  ( $\sim 10^{15} \text{ eV ng}^{-1}$ ). Additionally, a comparison between IR spectra from the laboratory and several YSOs suggests that the initial composition of grains in young stellar discs may include a mixture of  $\text{H}_2\text{O}$ ,  $\text{NH}_3$ , CO (or  $\text{CO}_2$ ), alkanes and  $\text{CH}_3\text{OH}$ . The  $7.7 \mu\text{m}$  ( $1300 \text{ cm}^{-1}$ ) feature in YSOs, which is attributed to  $\text{CH}_4$  ( $-\text{CH}$  deformation mode; Boogert *et al.* 1997), was best represented by the products coming from the radiolysis of ices initially containing alkanes, rather than by the ices where the primary source of carbon comes from CO. This suggests that saturated hydrocarbons, such as cyclohexane, may be a part of the initial chemical inventory of interstellar ices. However, the presence of broad features at  $1450$  and  $1680 \text{ cm}^{-1}$  in the astronomical observations, similar to the features observed in the IR spectra of the irradiated  $\text{H}_2\text{O}:\text{NH}_3:\text{CO}$  ice (Pilling *et al.* 2010a), requires the presence of CO (or/and  $\text{CO}_2$ ) as one of the parental species in the interstellar medium.

#### 4. Concluding remarks

In this work, we present some highlights of experiments employing swift ions broadband X-rays (plus fast electrons, low energy secondary electrons and a minor component of VUV photons) in astrophysical ices simulated in laboratory. The sample was analyzed by Fourier transform infrared spectroscopy FTIR at different radiation fluences. The experiments occurred at to laboratories in two countries: the Brazilian synchrotron light source (LNLS/CNPEM) in Campinas/Brazil and the Grand Accélérateur d'Ion Lourdes (GANIL/CIRIL/CIMAP) in Caen/France employing a similar methodology.

The selected results presented showed the interaction between cosmic ray analogs and ionizing soft X-rays probed in the laboratory and allow us to identify reaction routes that lead to chemical enhancement of astrophysical ices. For example, cosmic rays can induce the formation of alkenes and aromatic compounds (with eventual  $\text{H}_2$  release to the gas phase) during the irradiation of saturated hydrocarbon-containing ices, as well as the formation of peptide bonds in ices containing amino acids. Such organic compound production was also observed during the processing of  $\text{N}_2:\text{CH}_4$  ices by soft X-rays with the appearance of the nucleobase adenine, among the products of sample irradiation.

The results employing bombardment of astrophysical ice analogs by swift ions indicated that cosmic ray bombardment of saturated alkanes can be an alternative scenario for the production of unsaturated hydrocarbons and possibly aromatic rings (via dehydrogenation processes) in interstellar and protostellar ices. The results also indicate that a comparison between the laboratory spectra and IR observations of protostellar ices

suggest that saturated hydrocarbons such as cyclohexane may be a part of the initial chemical inventory of interstellar ices.

The determination of the effective destruction and formation cross section in solid state, allows us to estimate the molecular half-life extrapolated for astrophysical environments and help us put constraints also in prebiotic chemistry that may have triggered life to arise in the Early Earth.

### Acknowledgements

The author acknowledges the Brazilian agencies FAPESP (Projects JP 2009/18304-0, IC 2014/08643-0, DR 2012/17248-2 and MS 2016/11334-5) and CNPq (Research fellowship 304130/2012-5 and 306145/2015-4) as well as FVE/UNIVAP for the financial support. A special thank are given to the staff of UNIVAP and LNL/CNPEM and GANIL/CIRIL/CIMAP for the technical support and help during the experiments.

### References

- Akerman, A., Breskin, A., Chechik, R., & Gibrekhterman, A. 1993, in *Ionization of Solids by Heavy Particles*, ed. R. A. Baragiola, (Berlin: Springer), Vol. 306, 359
- Almeida, G. C., Pilling, S., Andrade, D. P. P., et al. 2014, *JPCC*, 118, 6193
- Almeida, G. C., Pilling, S., de Barros, A. L. F., da Costa, C. P., Pereira, R. C., & da Silveira, E. F. 2017, *MNRAS*, 471, 1330
- Andrade, D. P. P., de Barros, A. L. F., Pilling, S., Domaracka, A., Rothard, H., Boduch, P., & da Silveira, E. F. 2013, *MNRAS*, 787, 796
- Baragiola, R. A., Vidal, R. A., Svendsen, A., Schou, J., Shi, M., Bahr, D. A., & Atteberry, C. L. 2003, *Nuclear Instruments and Methods in Physics Research B*, 209, 294
- Bergantini, A., Pilling, S., Rothard, H., Boduch, P., & Andrade, D. P. P. 2014a, *MNRAS*, 437, 2720
- Bergantini, A., Pilling, S., Nair, B. G., Mason, N. J., & Fraser H. J. 2014b, *A&A*, 570, A120
- Bernstein, M. P., Dworkin, J. P., Sandford, S. A., et al. 2002, *Nature*, 416, 401
- Bonfim, V. S., Castilho, R. B., Baptista, L., & Pilling, S. 2017, *PCCP*, Accepted
- Boogert, A. C. A., Schutte, W. A., Helmich, F. P., Tielens, A. G. G. M., & Wooden, D. H. 1997, *A&A*, 317, 929
- Boogert, A. C. A., Pontoppidan, K. M., Lahuis, F., et al. 2004, *ApJS*, 154, 359
- Brown, W. L., Augustyniak, W. M., Marcantonio, K. J., et al. 1984, *Nucl. Instr. Meth. B1*, IV, 307
- Cazaux, J. 2006, *NIMPB*, 244, 307
- Chan, W. F., Cooper, G., & Brion, C. E. 1993, *Chem. Phys.*, 178, 387
- Chen, Y.-J., Ciaravella, A., Munõz Caro, G. M., et al. 2013, *ApJ*, 778, 162
- de Barros, A. L. F., da Silveira, E. F., Pilling, S., Domaracka, A., Rothard, H., & Boduch, P. 2014, *MNRAS* 483, 2026
- Dartois, E., Augé, B., Boduch, P., et al., 2015, *A&A*, 576, A125
- Ehrenfreund, P. & Charnley, S. B. 2000, *ARA&A*, 38, 427
- Gibb, E. L., Whittet, D. C. B., & Chiar, J. E. 2001, *ApJ*, 558, 702
- Gullikson, E. M. & Henke, B. L. 1989, *PhRvB*, 39, 1
- Henke, B. L., Liesegang, J., & Smith, S. D. 1979, *PhRvB*, 19, 3004
- Hijazi H., Rothard, H., Boduch, P., Alzahr, I., Ropars, F., et al. 2011, *Nucl. Instr. Meth. Phys. Res. B*, 269, 1003
- Hüfner, S. 1995, *Photoelectron Spectroscopy: Principles and Applications* (Berlin: Springer)
- Jimenez-Escobar A., Chen, Y.-J., Ciaravella, A., Huang, C.-H., Micela, G., & Cecchi-Pestellini, C. 2016, *ApJ*, 820, 25
- Kaiser, R. I., Stockton, A. M., Kim, Y. S., Jensen, E. C., & Mathies, R. A. 2013, *AJ*, 765, 111
- Kobayashi, K., Kaneko, T., Takano, Y., et al. 2008, *Proc. IAU Symp.* 251, 465
- Li A., Greenberg J. M. 1997, *A&A*, 323, 566
- Maloney, P. R., Hollenbach, D. J., & Tielens, A. G. G. M. 1996, *ApJ*, 466, 561

- McLaren, R., Ishii, I., Hitchcock, A. P., *et al.* 1987, *J. Chem. Phys.*, 87, 4344
- Mejía C., de Barros, A. L. F., Seperuelo Duarte, E., da Silveira, E. F., Dartois, E., Domaracka, A., Rothard, H., & Boduch, P. 2014, *Icarus*, 250, 222
- Mejía C., Bender, M., Severin, D., *et al.* 2015, *Nucl. Instrum. Meth. B*, 353, 477
- Muñoz Caro, G. M., Meierhenrich, U. J., Schutte, W. A., *et al.* 2002, *Nature*, 416, 403
- Öberg, K. I., van Dishoeck, E. F., & Linnartz, H. 2009, *A&A*, 496, 281
- Palumbo, M. E. 2006, *A&A*, 453, 903
- Pilling, S., Andrade, D. P. P., Neto, A. C., Rittner, R., & Brito A. N. 2009, *JPCA*, 113, 11161
- Pilling, S., Seperuelo Duarte, E., da Silveira, E. F., Balanzat, E., Rothard, H., Domaracka, A., & Boduch, P. 2010a, *A&A*, 509, A87
- Pilling, S., Seperuelo Duarte, E., Domaracka, A., Rothard, H., Boduch, P., & da Silveira, E. F. 2010b, *A&A*, 523, A77
- Pilling, S., Seperuelo-Duarte, E., Domaracka, A., Rothard, H., Boduch, P., & da Silveria E. F. 2011a, *PCCP*, 13, 15755
- Pilling, S., Andrade, D. P. P., do Nascimento, E. M., Marinho, R. R. T., Boechat-Roberty, H. M., de Coutinho, L. H., de Souza, G. G. B., de Castilho, R. B., Cavasso-Filho, R. L., Lago, A. F., & de Brito A. 2011b, *MNRAS*, 411, 2214
- Pilling, S. & Andrade, D. P. P. 2012, in *X-Ray Spectroscopy*, ed. S. K. Sharma (*Rijeka: InTech*), 185
- Pilling, S., Andrade, D. P. P., da Silveira, E. F., Rothard, H., Domaracka, A., & Boduch, P. 2012, *MNRAS*, 423, 2209
- Pilling, S., Mendes, L. A. V., Bordalo, V., Guaman, C. F. M., Ponciano, C. R., & da Silveira, E. F. 2013, *Astrobology*, 13, 79
- Pilling, S., Nair, B. G., Escobar, A., Fraser, H., & Mason, N. 2014, *EPJD*, 68, 58
- Pilling S. & Bergantini A. 2015, *ApJ*, 811, 151
- Portugal, W., Pilling, S., Boduch, P., Rothard, H., & Andrade, D. P. P. 2014, *MNRAS*, 441, 3209
- Prasad, S. S. & Tarafdar, S. P. 1983, *ApJ*, 267, 603
- Rachid, G. M., Faquine, K., & Pilling, S. 2017, *PSS*, In press, DOI: 10.1016/j.pss.2017.05.003
- Reis, E. F., Campos, F. S., Lage, A. P., Leite, R. C., Heneine, L. G., Vasconcelos, W. L., Lobato, Z. I. P., & Mansur, H. S. 2006, *Materials Res.*, 9, 185
- Shen, C. J. & Greenberg, J. M., Schutte W. A. 2004, *A&A*, 415, 203
- Seperuelo-Duarte, E., Boduch, P., Rothard, H., Been, T., Dartois, E., Farenzena, L. S., & da Silveira, E. F. 2009, *A&A*, 502, 599
- Seperuelo-Duarte, E., Domaracka, A., Boduch, P., Rothard, H., Dartois, E., & da Silveira, E. F. 2010, *A&A*, 512, A71.
- Strazzulla, G., Pirronello, V., & Foti, G. 1983, *ApJ*, 271, 255
- Strazzulla, G., Leto, G., Spinella, F., & Gomis, O. 2007, in *Kuhs W. F., ed., Proc. 11th Int. Conf. on the Physics and Chemistry of Ice. Royal Society of Chemistry, Cambridge*, p. 561
- Taylor, A. D., Baggaley, W. J., & Steel, D. I. 1996, *Nature*, 380, 323
- Vasconcelos, F. A., Pilling, S., Rocha, W. R. M., Rothard, H., Boduch, P., & Ding, J. J. 2017a, *Phys. Chem. Chem. Phys.*, 19, 12845
- Vasconcelos, F. A., Pilling, S., Rocha, W. R. M., Rothard, H., & Boduch, P. 2017b, *Phys. Chem. Chem. Phys.*, 19, 24154
- Vasconcelos, F. A., Pilling, S., Rocha, W. R. M., Rothard, H., & Boduch, P. 2017c, *ApJ*, submitted.
- Witt, A. N., Smith, R. K., & Dwek E. 2001, *ApJ*, 550, L201